Proceedings, 2004 International Conference on Slopeland Disaster Mitigation,
Taipei, Taiwan, October 5-6, 11 p.

Response of the Gravel Bed of a Mountain River to a Hydrograph

Gary Parker[1]

Mountain gravel-bed rivers typically display a surface layer that is armored. That is, the surface layer displayed at low flow is coarser than both the substrate and mean annual bedload transported. The surface layer is difficult to sample at the high flows that transport most of the gravel. As a result, the question as to whether the surface layer remains armored at high flows is something of a mystery. The few measurements available suggest that some form of armoring may be in place at high flows as well. In lieu of more measurements, numerical modeling provides an avenue to explore this issue. Research is presented on 1D modeling of aggradation and degradation to mobile-bed equilibrium in gravel-bed streams. In the model, a hydrograph is cycled repeatedly so that water discharge goes up and down in time. The magnitude of the bedload feed rate and the size distribution of the feed material are, however, held constant at the upstream end of the reach. As a result, the final mobile-bed equilibrium attained is characterized by a bed at the upstream end of the reach that cyclically degrades and coarsens at high flow (when the sediment feed rate is not sufficient) and aggrades and becomes finer at low flow (when there is an excess of sediment feed). Only a short distance downstream, however, a remarkable tradeoff occurs. The bed adjusts so that over the great majority of the modeled reach the bed elevation and surface size distribution become invariant, hardly changing at all from low flow to high flow. The bedload transport rate and size distribution, however, fluctuate strongly with the hydrograph. That is, the higher flows support a higher transport rate of coarser material and the lower flows support a lower transport rate of finer material. The implication is that rivers subject to repeated hydrographs can evolve so that neither surface grain size distribution nor mean bed elevation (averaged over bars) need change much with flow, nearly all the variation being absorbed by the bedload. If this is true, it provides a most useful result; the surface grain size distribution seen at low flow may be very close to that seen at high flow.

Keywords: rivers, gravel, armor, hydrograph

Introduction

Mountain gravel-bed rivers usually display a surface armor at low flow. That is, the size distribution of the surface material tends to be notably coarser than that of the substrate below. An example of this is shown for the River Wharfe, U.K. in Figure 1.

The grain size distribution of the surface layer during floods that actually move gravel remains something of a mystery. It is very difficult, and often dangerous to sample the bed of gravel-bed streams during floods. An example of a gravel-bed river at low flow and in flood is given in Figs. 2a,b. Experiments at laboratory scale by Parker *et al.* (1982a, 1982b), and more recently by Wilcock *et al.* (2001) indicate, however, that the armor persists in some form at high flow. In addition, field data collected by Andrews (1983) for Sagehen Creek, USA also indicate the persistence of armor at high flow.

The issue is of some importance because many of the more recent relations for the transport of size mixtures in gravel-bed streams are surface-based. That is, it is necessary to know the

[1] St. Anthony Falls Laboratory, University of Minnesota, 2 3rd St. Minneapolis MN 55414 USA parke002@umn.edu

size distribution of the bed surface (in addition to the flow over the surface) in order to predict the magnitude and size distribution of the bedload transport. Examples of such surface-based relations are those of Parker (1990) and Wilcock and Crowe (2003).

Fig. 1. Bed sediment of the River Wharfe, U.K., showing a pronounced surface armor. Image courtesy D. Powell.

a) b)

Fig. 2. Elbow River, Canada at a) low flow and b) a 100-year flood. Image courtesy Alberta Research Council, Canada.

Surface-based bedload transport relations for gravel-bed rivers have been widely applied to cases for which either a) the flow discharge and surface size distribution are specified and the bedload transport rate and grain size distribution are calculated, or inversely b) the flow discharge, bedload transport rate and grain size distribution are specified and the associated surface size distribution is calculated (e.g. Parker, 1990). Rivers are not, however, subject to single discharges. Rather, they are subject to the repeat of similar hydrographs.

How does the bed surface evolve in response to repeated hydrographs? Here the question is addressed numerically in terms of a hydrograph that is repeated over and over again until the river bed evolves to a mobile-bed equilibrium (when averaged over the hydrograph). A somewhat surprising result is obtained. According to the results of the numerical model, the river evolves toward an equilibrium state for which the surface size distribution remains approximately constant over the hydrograph.

Configuration of the numerical experiments

The river reach under consideration has length L and constant width B, as illustrated in Fig. 3. The river has no floodplain in the calculation presented here. The bed surface (active, exchange) layer has thickness L_a. The volume fraction of material in the ith grain size range in the surface layer is denoted as F_i. The substrate size fractions f_i are approximated as constant everywhere, but the surface fractions $F_i(x, t)$ are, as indicated, functions of streamwise distance x and time t.

The river is assumed to be sufficiently steep to allow for the neglect of backwater effects. The flood wave associated with changed discharge is assumed to be sufficiently fast compared with times for significant morphological evolution of the bed that at any given time the water discharge Q is the same everywhere.

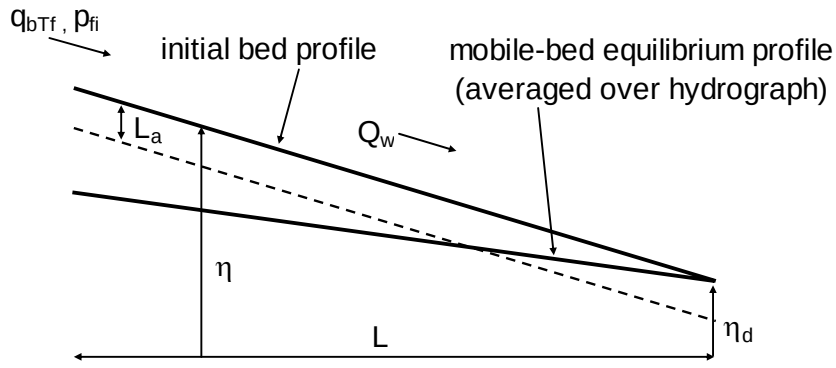

Fig. 3. Definition diagram for the numerical experiments.

The volume bedload transport rate per unit width in the ith grain size range is denoted as q_{bi}; in general, it is a function of x and t. The total volume bedload transport rate per unit width summed over all grain sizes is denoted as q_{bT}, where

$$q_{bT} = \sum_{i=1}^{N} q_{bi} \qquad 1$$

and N denotes the number of grain sizes needed to specify the available material. The volume fraction of bedload material in the ith grain size is then given as

$$p_i = \frac{q_{bi}}{q_{bT}} \qquad 2$$

In the calculations presented here, the flow hydrograph is specified in terms of w steps, each having duration Δt_w and water discharge Q_w, w = 1..W (Fig. 4). The same hydrograph is repeated until mobile-bed equilibrium is reached. The sediment feed rate q_{bTf} and feed fractions p_{fi} are, however, identical for every step in the hydrograph. In addition, the substrate fractions f_i are specified constants. The hydrograph is repeated until the reach again reaches a mobile-bed equilibrium (averaged over the hydrograph). The goal is to see how the surface size distribution varies with discharge within the hydrograph after this mobile-bed equilibrium has been reached.

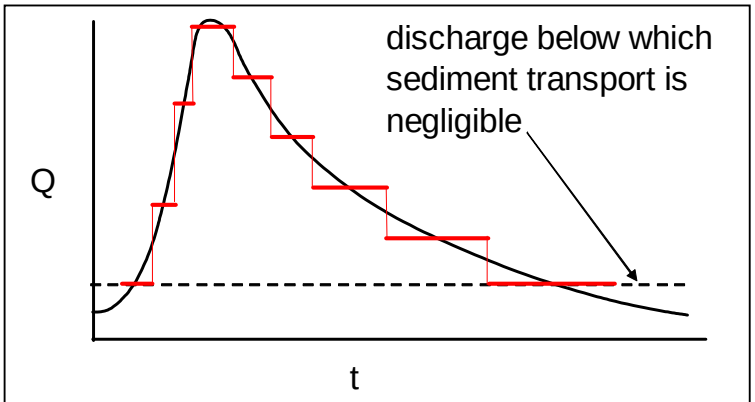

Fig. 4. Discretization of the flow hydrograph.

The results of 11 numerical experiments are reported here. The flow hydrograph is identical in all 11 runs. The size distribution of the sediment feed is the same for every step of the hydrograph of each run, and indeed is the same for each run. The sediment feed rate is the same for every step of the hydrograph for each run, but varies from run to run.

Exner equation of sediment conservation for mixtures

Evolution of the bed toward mobile-bed equilibrium is modeled using the Exner equation of sediment conservation for mixtures. This relation defines how bed elevation $\eta(x, t)$ and surface grain size fractions $F_i(x, t)$ vary in response to differential transport of sediment mixtures. As equilibrium is approached, the reach evolves to one for which the bed slope $S = -\partial\eta/\partial x$ and surface fractions F_i evolve toward values that are invariant when averaged over the hydrograph.

The following parameters are defined: x = streamwise distance, t = time, η = bed elevation, L_a = thickness of the surface (active, exchange) layer, λ_p = bed porosity, D_i = size of the ith grain size in the mixture, F_i = volume fraction of material in the surface layer in the ith grain size range and q_{bi} = the volume bedload transport rate in the ith grain size range. The Exner equation of sediment conservation for sediment mixtures takes the form

$$(1-\lambda_p)\left[f_{Ii}\frac{\partial}{\partial t}(\eta - L_a) + \frac{\partial}{\partial t}(F_i L_a)\right] = -\frac{\partial q_{bi}}{\partial x} \qquad 3$$

where f_{Ii} is an interfacial fraction of material that is exchanged between the surface layer and the substrate as the bed aggrades or degrades (e.g. Parker, 1991). Here these fractions are specified as

$$f_{Ii} = \begin{cases} f_i\big|_{z=\eta-L_a}, & \dfrac{\partial\eta}{\partial t} < 0 \\ \alpha F_i + (1-\alpha)p_i, & \dfrac{\partial\eta}{\partial t} > 0 \end{cases} \qquad 4$$

where f_i denotes the fractions in the substrate, p_i denotes the fractions in the bedload, given according to (2), and α is a constant between 0 and 1 (e.g. Toro-Escobar *et al.* 1996). In the runs reported here λ_p is set equal to 0.4 and α is set equal to 0.5.

The parameters F_i, f_{Ii}, f_i and p_i must sum to unity over all grain sizes; e.g.

$$\sum_{i=1}^{N} F_i = 1 \qquad 5$$

Summing (1) over all grain sizes results in a version of the Exner equation suitable for computing streambed elevation variation as a function of differential sediment transport:

$$(1-\lambda_p)\frac{\partial\eta}{\partial t} = -\frac{\partial q_{bT}}{\partial x} \qquad 6$$

Between (1) and (5) the following equation describing the evolution of the surface size distribution is obtained:

$$(1-\lambda_p)\left[L_a\frac{\partial F_i}{\partial t} + (F_i - f_{Ii})\frac{\partial L_a}{\partial t}\right] = -\frac{\partial q_{bT} p_i}{\partial x} + f_{Ii}\frac{\partial q_{bT}}{\partial x} \qquad 7$$

In the implementation of the Exner formulation described below, the following relation is used for L_a;

$$L_a = 2D_{90} \qquad 8$$

where D_{90} denotes the size such that 90 percent of the surface material is finer.

Sediment transport relation and hydraulic modeling

The sediment transport relation used in the formulation is that of Wilcock and Crowe (2003). It takes the form

$$\frac{Rgq_{bi}}{F_i u_*^3} = G(\phi) \qquad 9a$$

where

$$G = \begin{cases} 0.002\phi^{7.5} & \text{for } \phi < 1.35 \\ 14\left(1 - \frac{0.894}{\phi^{0.5}}\right)^{4.5} & \text{for } \phi \geq 1.35 \end{cases}$$

$$\phi = \frac{\tau^*_{s50}}{\tau^*_{ssr50}}\left(\frac{D_i}{D_{50}}\right)^{-b} \qquad 9b,c,d,e$$

$$\tau^*_{ssr50} = 0.021 + 0.013\exp(-14F_s)$$

$$b = \frac{0.69}{1 + \exp(1.5 - D_i / D_{50})}$$

In the above relations g denotes gravitational acceleration, D_{50} denotes the median size of the surface material, F_s denotes the volume fraction of surface material that is sand (rather than gravel) and R denotes the submerged specific gravity of the sediment, given as

$$R = \frac{\rho_s}{\rho} - 1 \qquad 10$$

where ρ_s and ρ denote the densities of the sediment and water, respectively. For natural sediment R is usually close to 1.65. In addition τ^*_{s50} denotes a Shields number and u_* denotes a shear velocity, given by the relations

$$\tau^*_{s50} = \frac{HS}{RD_{50}} \quad , \quad u_* = \sqrt{gHS} \qquad 11a,b$$

where H denotes depth and S denotes bed slope.

The formulation for sediment transport must be augmented by a corresponding formulation for flow hydraulics. Here the hydraulics are approximated as normal flow. The equation of water continuity can be written for any discharge Q as

$$Q = UBH \qquad 12$$

where H denotes flow depth and U denotes the depth-averaged flow velocity. Flow momentum balance is expressed as a simple balance between the dowstream pull of gravity and the resistive force on the bed:

$$C_f U^2 = gHS \qquad 13$$

where the dimensionless friction coefficient C_f is given by the Manning-Strickler relation of Parker (1991);

$$C_f^{-1/2} = 8.1\left(\frac{H}{k_s}\right)^{1/6} \quad , \quad k_s = 2D_{90} \qquad 14a,b$$

In the above relations k_s denotes a roughness height and D_{90} denotes the size such that 90 percent of the surface material is finer.

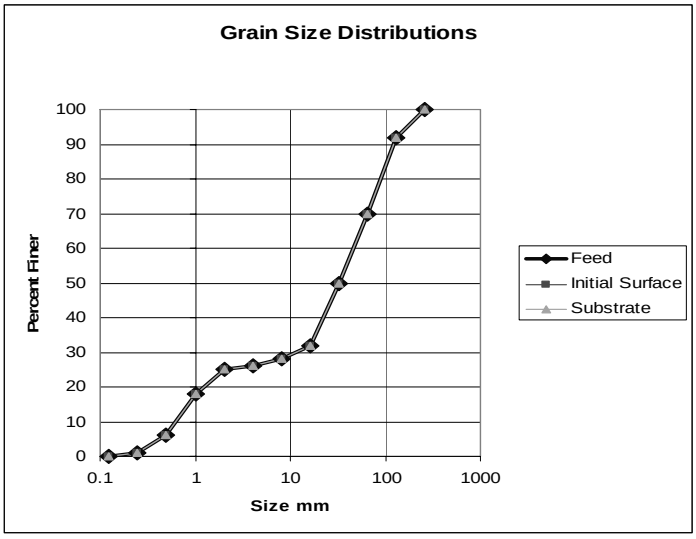

Fig. 5. Grain size distributions.

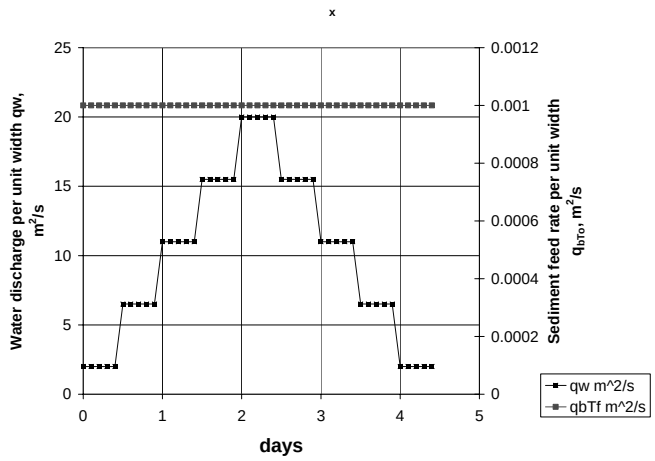

Fig. 6. Flow hydrograph.

Input parameters

The grain size distributions of the sediment feed, substrate and initial surface layer are specified in Fig. 5; they are identical. The grain size distribution of the sediment feed is the same for every step of the hydrograph in the runs reported here, and indeed is the same for every run. The feed sediment is 75 percent gravel and 25 percent sand.

The volume total sediment feed rate per unit width q_{bTf} is held constant for each run. Results for 11 runs are reported, with q_{bTf} varying from $1x10^{-6}$ m^2/s to $1x10^{-1}$ m^2/s. The flow hydrograph consists of 9 steps, each lasting 0.5 days, for a total of 4.5 days. This hydrograph is repeated once each year. Since channel width B is constant, discharge for each step is specified in terms of water discharge per unit width q_w, where

$$Q = q_w B \qquad 15$$

The hydrograph is given in Fig. 6. It is identical for the 11 runs reported here.

Reach length L was set equal to 20 km. The downstream boundary condition was one of constant bed elevation (Fig. 3), so that

$$\eta_d = \eta(L,t) = 0 \qquad 16$$

The initial bed slope was varied from run to run so as to reduce the time required to mobile-bed equilibrium. This time typically varied in the range of hundreds to tens of thousands of years, the larger value corresponding to the lower feed rates.

Results

Fig. 7 shows plots three parameters as functions of the total sediment feed rate q_{bTf}; surface geometric mean size, bedload geometric mean size, and bed slope. Also included is the geometric mean size of the feed All parameters pertain to the downstream end of the reach, and are averaged over the final hydrograph of the run.

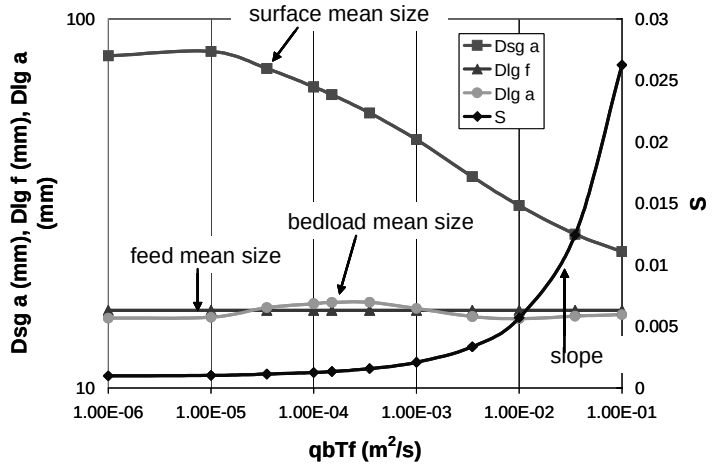

Fig. 7. Surface geometric mean size, bedload geometric mean size and bed slope, all averaged over the hydrograph for the last hydrograph of the run, as functions of bedload feed rate q_{bTf}. The values pertain to the downstream end of the reach. Virtually identical patterns are obtained everywhere except very near the sediment feed point. The geometric mean size of the sediment feed is included for reference.

It is seen in Fig. 7 that the bedload geometric mean size is nearly constant, and is very close to the value for the sediment feed. This indicates that mobile-bed equilibrium was indeed reached. At this mobile-bed equilibrium, however, the surface geometric mean size systematically decreases with increasing sediment feed rate. The implication is a very well-developed surface armor at a feed rate of $1x10^{-6}$ m^2/s, and much less armouring at a feed rate of $1x10^{-1}$ m^2/s. Fig. 7 also shows a tendency for equilibrium bed slope to increase with feed rate. That is, a higher feed rate results in a higher equilibrium bed slope.

Although the results in Fig. 7 are specifically for the downstream end of the reach, it should be noted that virtually the same results are obtained at mobile-bed equilibrium everywhere except in a short subreach near the feed point. This also holds true for Figs. 8 and 9 below. The meaning of this result is explained in more detail below.

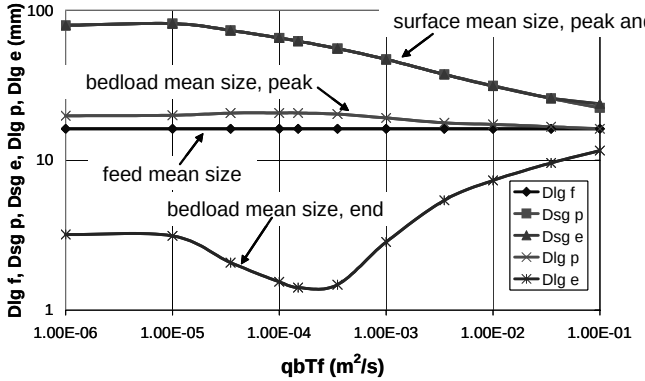

Fig. 8. Surface geometric mean size and bedload geometric mean size at a) the peak (maximum) flow of the last hydrograph of the run and b) the end (low) flow of the last hydrograph of the run as functions of the feed rate q_{bTf}. The values pertain to the downstream end of the reach. Virtually identical patterns are obtained everywhere except very near the sediment feed point. The geometric mean size of the sediment feed is included for reference.

Fig. 8 shows the geometric mean sizes of a) the surface and b) the bedload at both the peak flow of the hydrograph and the end (low) flow of the hydrograph. The hydrograph in question is the last one of the run, i.e. after mobile-bed equilibrium had been reached. The parameters pertain to the downstream end of the reach.

Fig. 8 shows a remarkable characteristic. The geometric mean size of the bedload at the peak flow is invariably considerably larger than that at the end (low) flow. The geometric mean size of the surface is, however, virtually identical at the peak and end flows. The

implication is that the bed surface has evolved so that it no longer varies with the hydrograph once mobile-bed equilibrium is reached.

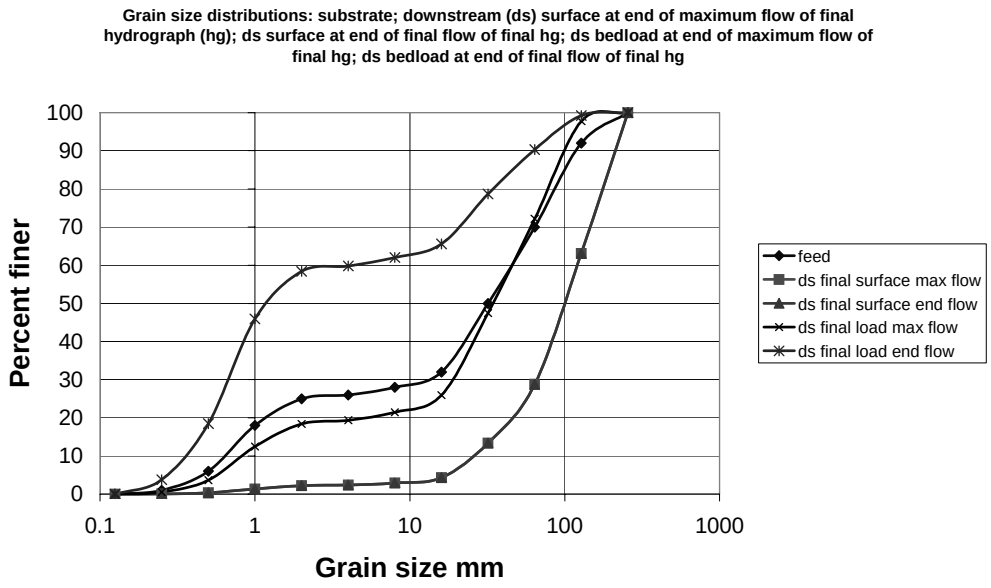

Fig. 9a. Grain size distributions of a) the surface at the peak (maximum) flow of the hydrograph, b) the surface at the end (low) flow of the hydrograph, c) the bedload at the peak (maximum) flow of the hydrograph, and d) the bedload at the end (low) flow of the hydrograph. The values are for a feed rate q_{bTf} of $1x10^{-6}$ m^2/s. They pertain to the last hydrograph of the run and the downstream end of the reach. Virtually identical results are obtained, however, for all points except very near the upstream end. The grain size distribution of the feed is included for reference.

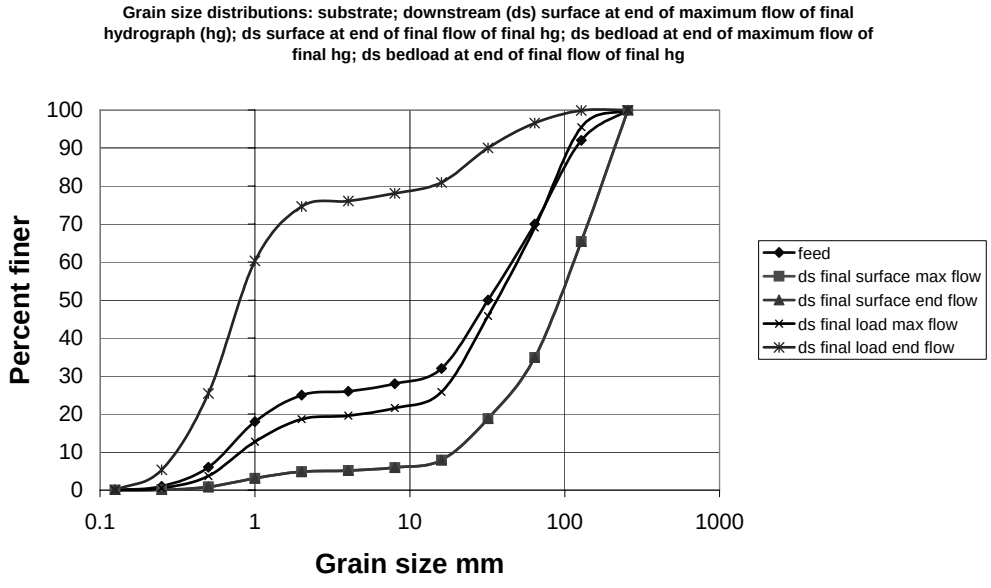

Fig. 9b. Grain size distributions of a) the surface at the peak (maximum) flow of the hydrograph, b) the surface at the end (low) flow of the hydrograph, c) the bedload at the peak (maximum) flow of the hydrograph, and d) the bedload at the end (low) flow of the hydrograph. The values are for a feed rate q_{bTf} of $1x10^{-4}$ m^2/s. They pertain to the last hydrograph of the run and the downstream end of the reach. Virtually identical results are obtained, however, for all points except very near the upstream end. The grain size distribution of the feed is included for reference.

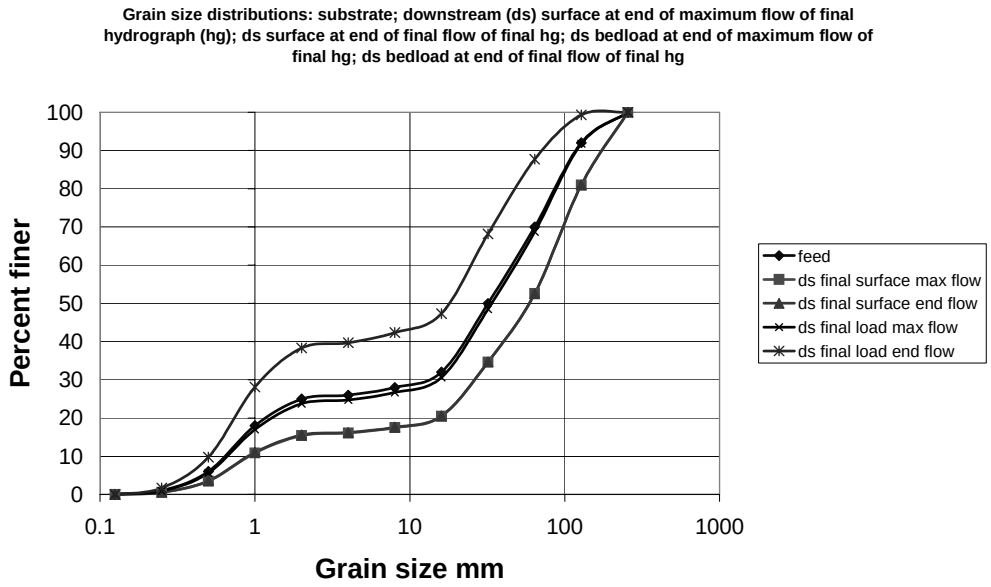

Fig. 9c. Grain size distributions of a) the surface at the peak (maximum) flow of the hydrograph, b) the surface at the end (low) flow of the hydrograph, c) the bedload at the peak (maximum) flow of the hydrograph, and d) the bedload at the end (low) flow of the hydrograph. The values are for a feed rate q_{bTf} of $1x10^{-2}$ m^2/s. They pertain to the last hydrograph of the run and the downstream end of the reach. Virtually identical results are obtained, however, for all points except very near the upstream end. The grain size distribution of the feed is included for reference.

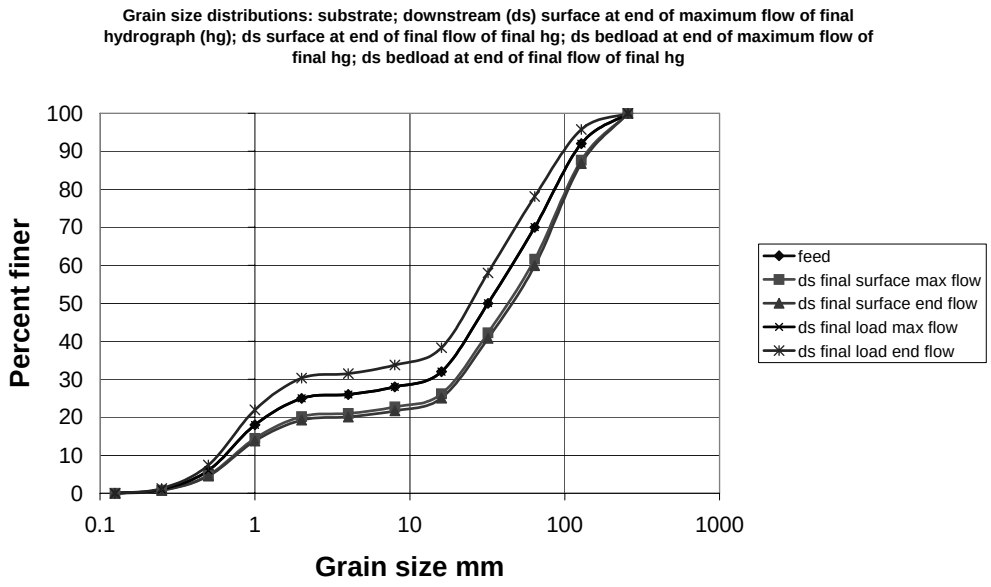

Fig. 9d. Grain size distributions of a) the surface at the peak (maximum) flow of the hydrograph, b) the surface at the end (low) flow of the hydrograph, c) the bedload at the peak (maximum) flow of the hydrograph, and d) the bedload at the end (low) flow of the hydrograph. The values are for a feed rate q_{bTf} of $1x10^{-1}$ m^2/s. They pertain to the last hydrograph of the run and the downstream end of the reach. Virtually identical results are obtained, however, for all points except very near the upstream end. The grain size distribution of the feed is included for reference.

Indeed, it is found that the same condition at mobile-bed equilibrium holds throughout the reach with the exception of a short region near the sediment feed point. This behaviour can be explained as follows.

Even at mobile-bed equilibrium, the grain size distribution of the surface layer must vary over the hydrograph at or very near the feed point. This is because the sediment feed rate is held constant over the hydrograph, but the flow discharge is changing. At the high flows the feed rate is less than the capacity transport rate: the bed degrades and coarsens. At the low flows the feed rate is greater than the capacity rate: the bed aggrades and becomes finer. At mobile-bed equilibrium this pattern repeats cyclically.

A tradeoff occurs, however, in the downstream direction. The bed size distribution is able to adjust itself so that it no longer changes significantly with discharge within the hydrograph. Instead, the magnitude and size distribution of the bedload absorb the change. The result is a bed surface elevation and size distribution that are nearly invariant with flow within the hydrograph, but a bedload transport rate and size distribution that vary significantly with flow within the hydrograph.

Figures 9a-d show grain size distributions of a) the feed sediment, b) the surface at the peak (maximum) flow of the hydrograph, c) the surface at the end (low) flow of the hydrograph, d) the bedload at the peak (maximum) flow of the hydrograph and e) the bedload at the end (low) flow of the hydrograph, for the four sediment feed rates $q_{bTf} = 1x10^{-6}$ m^2/s, $1x10^{-4}$ m^2/s, $1x10^{-2}$ m^2/s and $1x10^{-1}$ m^2/s. All distributions pertain to the last hydrograph of the run, by which time mobile-bed equilibrium has been reached, and the downstream end of the reach. These plots verify that the surface size distributions at the end (low) flow are virtually identical to those at the peak (maximum) flow. The only deviation from this pattern occurs for the very highest sediment feed rate, and the deviation is slight. The bedload size distribution at the end (low) flow is, however, systematically finer than that at the peak (maximum) flow. The difference between the two is least for the highest sediment feed rate. It can be seen from the figures that for the highest feed rate a) the armor is least developed relative to the sediment feed and b) the bedload size distribution at the peak flow differs least from that at the end flow.

Conclusions

The numerical runs reported here provide a strong argument for the concept that gravel-bed rivers in a given hydrologic regime evolve to a mobile-bed equilibrium at which the bed slope and surface size distribution vary little with flow, and the bedload transport and size distribution vary strongly with flow. At mobile-bed equilibrium the surface size distribution for a given hydrologic regime does become systematically finer, and the bed slope higher, as the sediment feed rate increases.

These results could prove quite useful. In applying a surface-based bedload transport equation to flood flows, it may be sufficient to use a surface grain size distribution measured at low flow.

The research for this paper was supported by the National Center for Earth-surface Dynamics, which in turn funded by the Science and Technology Center program of the National Science Foundation of the USA. It represents a contribution in the area of a) river restoration and b) channel dynamics. Marwan Hassan and Peter Wilcock greatly aided in the formulation of the research.

References

Andrews, E. D. 1983. Entrainment of gravel from naturally sorted riverbed materials. Geological Society of America Bulletin, 94, pp. 1225-1231.

Parker, G., S. Dhamotharan, and S. Stefan 1982a. Model experiments on mobile, paved gravel bed streams. Water Resources Research, 18(5), pp. 1395-1408.

Parker, G. and P. C. Klingeman 1982b. On why gravel bed streams are paved. Water Resources Research, 18(5), pp. 1409-1423.

Parker, G. 1990. Surface-based bedload transport relation for gravel rivers. Journal of Hydraulic Research, 28(4), pp. 417-436.

Parker, G. 1991. Selective sorting and abrasion of river gravel. I: Theory. Journal of Hydraulic Engineering, 117(2), pp. 131-149.

Toro-Escobar, C. M., G. Parker and C. Paola. 1996. Transfer function for the deposition of poorly sorted gravel in response to streambed aggradation. Journal of Hydraulic Research, 34(1), pp. 35-53.

Wilcock, P. R., S. T. Kenworthy and J. C. Crowe. 2001. Experimental study of the transport of mixed sand and gravel. Water Resources Research, 37(12), pp. 3349-3358.

Wilcock, P. R., and J. C. Crowe. 2003. Surface-based transport model for mixed-size sediment. Journal of Hydraulic Engineering, 129(2), pp. 120-128.